Derivative-free Kalman filtering based Approaches to Dynamic State Estimation for Power Systems with Unknown Inputs

Georgios Anagnostou, *Member, IEEE,* and Bikash C. Pal, *Fellow, IEEE*

***Abstract*—This paper proposes a decentralized derivative-free dynamic state estimation method in the context of a power system with unknown inputs, to address cases when system linearisation is cumbersome or impossible. The suggested algorithm tackles situations when several inputs, such as the excitation voltage, are characterized by uncertainty in terms of their status. The technique engages one generation unit only and its associated measurements, and it remains totally independent of other system wide measurements and parameters, facilitating in this way the applicability of this process on a decentralized basis. The robustness of the method is validated against different contingencies. The impact of parameter errors, process and measurement noise on the unknown input estimation performance is discussed. This understanding is further supported through detailed studies in a realistic power system model.**

***Index Terms*—Dynamic state estimation, Kalman filters, phasor measurements, power system dynamics, state estimation, synchronous generator, unscented transformation**

NOMENCLATURE

α	Difference between rotor angle and stator voltage phase in rad
χ	State sigma point
χ^b	Biased predicted state sigma point
χ^u	Unbiased predicted state sigma point
Δ	Linear regression model error term
δ	Rotor angle in rad
γ^b	Biased predicted measurement sigma point
γ^u	Unbiased predicted measurement sigma point
$\hat{d}$	Unbiased predicted unknown input
$\hat{x}^b$	Biased predicted state estimate
$\hat{x}^{u+}$	Unbiased a posteriori state estimate
$\hat{x}^{u-}$	Unbiased a priori state estimate
$\hat{y}^b$	Biased predicted measurement
$\hat{y}^u$	Unbiased predicted measurement
κ	Scaling parameter of sigma point spread
$\boldsymbol{n}$	Number of states in the augmented state vector
$\boldsymbol{P}$	Augmented state error covariance
$\boldsymbol{Q}$	Augmented additive process noise covariance
ω, ω_B	Rotor speed in p.u. and its base value in rad/s
ϕ_I	Stator current phase with respect to stator voltage phase in rad
ϕ_{Iy}	Measured stator current phase
ϕ	Difference between stator voltage and stator current phases in rad
ψ_{1d}	Subtransient emf due to d-axis damper coil in p.u.
ψ_{2q}	Subtransient emf due to q-axis damper coil in p.u.
$\mathbf{0}_{\alpha\times\beta}$	Zero matrix of size $(\alpha \times \beta)$
$\mathbf{x}$	Augmented state variables vector
θ	Stator voltage phase in rad
$\tilde{y}$	Measurement innovation
υ_f	Measurement noise associated with f_{sys_y}
υ_I	Measurement noise associated with I_y
υ_P	Measurement noise associated with P_y
υ_Q	Measurement noise associated with Q_y
υ_{ϕ_I}	Measurement noise associated with ϕ_{Iy}
υ	Column vector of measurement noise
c	Measurement equation approximation constant vector
D	Rotor damping constant in p.u.
d	Column vector of system unknown inputs
e	Measurement equation linearization error
E'_{dc}	Transient emf due to flux in q-axis dummy coil in p.u.
E'_d	Transient emf due to flux in q-axis damper coil in p.u.
E'_q	Transient emf due to field flux linkages in p.u.
E_{fd}	Generator field excitation voltage in p.u.
f	Discrete form of system differential equations
f_θ	Rate of change of the stator voltage phase in p.u.
f_υ	Noise term of the measured value of f_θ in p.u.
f_y	Measured value of f_θ in p.u.
f_{sys_y}	Measured system frequency
f_{sys}	System frequency in p.u.
G	Discrete form of unknown input distribution matrix
h	Column vector of system measurement equations
H_m	Measurement equation linear approximation
I	Stator current magnitude in p.u.
i	ith generator
I_d	d-axis component of the stator current in p.u.
I_q	q-axis component of the stator current in p.u.
I_y	Measured stator current magnitude
K	Kalman gain matrix
k	kth time step
K_{d1}	Ratio $(X''_d - X_{ls}) / (X'_d - X_{ls})$
K_{d2}	Ratio $(X'_d - X''_d) / (X'_d - X_{ls})$
K_{q1}	Ratio $\left(X''_q - X_{ls}\right) / \left(X'_q - X_{ls}\right)$
K_{q2}	Ratio $\left(X'_q - X''_q\right) / \left(X'_q - X_{ls}\right)$

This work has been supported by the Department of Electrical and Electronic Engineering, Imperial College London, and in part by U.K. –China initiative in Stability and Control of Power Networks with Energy Storage (STABLE-NET) funded by Research Councils U.K. (RCUK) Energy Programme in U.K. (Contract EP/L014343/1)

G. Anagnostou and B. C. Pal are with the Department of Electrical and Electronic Engineering, Imperial College London SW7 2AZ, U.K. (e-mails: georgios.anagnostou11@imperial.ac.uk; b.pal@imperial.ac.uk)

l	lth sigma point
M	Inertia constant in p.u.
m	Number of measurements
n	Number of state variables
p	Number of unknown inputs
P^b	Biased predicted state error covariance
P^{u+}	Unbiased a posteriori state error covariance estimate
P^{u-}	Unbiased a priori state error covariance estimate
P_x	State error covariance
P_y^u	Unbiased predicted measurement error covariance
$P_{w_p x}$	Cross-correlation between the nonlinear process noise and the states
P_{w_p}	Estimated nonlinear process noise covariance
P_{xy}^b	Biased cross-covariance between $\hat{x}^b$ and $\hat{y}^b$
P_{xy}^u	Unbiased cross-covariance between $\hat{x}^{u-}$ and $\hat{y}^u$
P_y	Measured active power value
Q	Constant additive process noise covariance
Q_p	Constant nonlinear process noise covariance
Q_y	Measured active power value
R	Measurement noise covariance
r	Number of (known) inputs
R_s	Armature resistance in p.u.
T	Matrix transpose
T'_{d0}	d-axis transient time constant
T'_{q0}	q-axis transient time constant
T_0	Simulation time step
T_e	Electrical torque input in p.u.
T_m	Mechanical torque input in p.u.
T''_d	d-axis subtransient time constant in s
T''_q	q-axis subtransient time constant in s
u	Column vector of system inputs
V	Stator voltage magnitude in p.u.
V_v	Noise term of the measured value of V in p.u.
V_y	Measured value of V in p.u.
W	Sigma point weight
w	Discrete form of process noise vector
w_p	Nonlinear process noise
x	Column vector of system state variables
X'_d	d-axis transient reactance in p.u.
X'_q	q-axis transient reactance in p.u.
X_d	d-axis synchronous reactance in p.u.
X_q	q-axis synchronous reactance in p.u.
X''_d	d-axis subtransient reactance in p.u.
X_{ls}	Armature leakage reactance in p.u.
X''_q	q-axis subtransient reactance in p.u.
y	Column vector of system measurements

I. Introduction

MODERN power systems are facing major operational challenges [1], driven by the rapid deployment of renewable energy based new generation technologies, increasing power consumption and limited investments in transmission level, leading to system operation close to its limits [2]. The arising complexity, as well as the experience from the 1996 North American Power Blackouts in WECC system [3] resulted in more sophisticated tools of capturing the system stability conditions and security margins, based on methods belonging to the area of *dynamic security assessment* (DSA) [4]. Operators' awareness of the power system state is very much dependent on wide area monitoring systems (WAMS). *Dynamic state estimation* (DSE), supported by WAMS, always provides useful outputs. In this context, Kalman filtering and its variants, such as the Extended Kalman filtering (EKF) and the Unscented Kalman filtering (UKF) have gained much popularity, since they can be applied to power systems, which are inherently characterized by nonlinearity [5], [6].

Kalman filtering based DSE requires good knowledge of the power system dynamic model. However, a centralized dynamic state estimation scheme would necessitate accurate information about all the states and devices of the system, as well as the phasor measurement unit (PMU) measurements across all the network, which is practically infeasible, especially for real-time implementations [7]. This fact has driven research in decentralized state estimation approaches [7]–[9]. Nevertheless, even in this case, the generation unit model is subjected to uncertainties. For instance, although excitation voltage measurement is possible through PMUs [5], [10], this is difficult to be applied in brushless excitation systems [6]. Moreover, under stressed conditions, the excitation voltage is likely to be dictated by timer-based overexcitation limiters, dramatically affecting the system stability margin [11]. Therefore, to tackle the cases of inaccessible or uncertain inputs in power system models, several dynamic state estimation algorithms have been employed, based on EKF [6], [9].

UKF has a proven superiority compared to EKF in terms of estimation accuracy in nonlinear systems [12]. In addition, contrary to EKF, this method does not involve Jacobian based linearisation, which can be rather complicated with regard to highly nonlinear systems, such as power networks [7]. Furthermore, system linearisation might be impossible when there are functions which are not smooth. In this context, this research study deals with the development of a derivative-free Kalman filtering based power system dynamic state estimation method with unknown (or inaccessible) inputs, assuming no prior knowledge of the unknown input models or distributions, in contrast with [7] for instance, where, in the proposed decentralized UKF algorithm, all system inputs were known. There have been similar research efforts in other fields, such as health assessment of structural systems [13], or control systems [14], [15], where linear relationship is inferred between the state variables and measurements. In [16], the nonlinear measurement equations are approximated using both linearisation and derivative-free techniques, but in this study there is a direct relationship between the unknown inputs and the measurement equations, which is not always the case in power systems. Here, this research effort leads to the following contributions:

- to establish a decentralized derivative-free Kalman filtering based dynamic state estimation framework for power systems with unknown inputs;
- to introduce a new synchronous generator model in the decentralized context, without any knowledge required from the network, apart from the information obtained by measurements at its terminal bus;
- to tackle nonlinearity in system measurement equations;

- to shed light on techniques to minimize the impact of measurement noise.

The remainder of this paper is organised as follows: In Section II, the proposed dynamic state estimation method is developed and analysed. Section III presents the generation unit model used in the decentralized state estimation context. Section IV includes the case studies evaluating the performance of the proposed method in a model power system: the IEEE benchmark 68-bus 16-machine system, representing the inter-connected New England (NETS) and New York (NYPS) power systems, which are connected to other three geographical regions [17], [18]. Section V discusses the effect of parameter errors, process and measurement noise on the state and unknown input estimation results, and this part also discusses techniques addressing the impact of measurement noise. Section VI concludes the paper.

II. Sigma-point based Kalman Filtering with Unknown Inputs

It assumed that the power system is described by the following set of discrete nonlinear differential-algebraic equations (DAEs):

$$\begin{aligned} x_k &= f\left(x_{k-1}, u_{k-1}, w_{k-1}\right) + G d_{k-1} \\ y_k &= h\left(x_k, u_k\right) + \upsilon_k \end{aligned} \tag{1}$$

where x and w are n-dimensional vectors of state variables and process noise, respectively, u is a r-dimensional vector of system (known) inputs, d is a p-dimensional vector of unknown inputs, y and υ are m-dimensional vectors of measurements and measurement noise, respectively, whereas, f and h denote the system dynamic and measurement equations, respectively, G is the unknown input distribution matrix, showing the relationship between the dynamic states and the unknown inputs, and k is the time step.

In this model, process and measurement noise vectors are supposed to be Gaussian, zero-mean, white, and uncorrelated to each other. This means that:

$$\begin{aligned} E[w_k \upsilon_k^T] &= E[\upsilon_k w_k^T] = 0 \text{ for all } k \\ E[w_k w_j^T] &= E[\upsilon_k \upsilon_j^T] = 0 \text{ for } k \neq j \\ E[w_k w_k^T] &= Q_k \\ E[\upsilon_k \upsilon_k^T] &= R_k \end{aligned} \tag{2}$$

The formulation of the unknown input estimation procedure is very similar to the ones used in [14], [15]. However, in these cases, the state variables of the systems are linearly related to the measurement outputs. Nonetheless, this is very difficult to appear in power system dynamic models. In order to overcome this bottleneck, the statistical linearisation approach is employed, which does not involve any calculation of derivatives [19]. The proposed method aims at joint state (x_k) and unknown input (d_{k-1}) estimation at every time step k. It has to be noted that at every time step, the unknown input of the previous time step is estimated (in contrast with the state variables' case), since there is no direct relationship between the unknown inputs and the measurement output equations.

The suggested algorithm is developed as follows:

A. Biased State Estimation

The starting point of every step is the biased dynamic state estimation, since there is no prior information regarding the unknown input of the previous step. The states are predicted as shown below:

1) Sigma point generation: Sigma point filters are based on the creation of a collection of points, capturing the several statistical properties of a random variable, and here the target is to obtain a good approximation of the mean and the covariance of x [20], [21]. Besides, the unscented transformation relies on a concept according to which it is easier to approximate a probability distribution than it is to approximate a nonlinear function [20]. The standard UKF employs the following set of sigma points [20]:

$$\begin{aligned} \chi_{k-1}^{(l)} &= \begin{bmatrix} \hat{x}_{k-1}^{u+} & \hat{x}_{k-1}^{u+} + \tilde{x}^{(l)} & \hat{x}_{k-1}^{u+} - \tilde{x}^{(l)} \end{bmatrix} \\ \tilde{x}^{(l)} &= \left(\sqrt{(n+\kappa) P_{k-1}^{u+}} \right)_l, \quad l = 1, 2, ..., n \end{aligned} \tag{3}$$

where $\hat{x}_{k-1}^{u+}$ and P_{k-1}^{u+} are the unbiased dynamic state estimate and the unbiased a posteriori state error covariance estimate of the previous time step, respectively, and κ is the scaling parameter of the spread of sigma points around $\hat{x}_{k-1}^{u+}$ [20]. Here, $\kappa = 3 - n$. Also, $\left(\sqrt{(n+\kappa) P_{k-1}^{u+}} \right)_l$ is the lth column of the lower triangular matrix resulting from the Cholesky decomposition: $(n+\kappa) P_{k-1}^{u+} = \sqrt{(n+\kappa) P_{k-1}^{u+}} \sqrt{(n+\kappa) P_{k-1}^{u+}}^T$.

2) Biased state prediction: Here, the sigma points are instantiated through the process model (i.e the dynamic state equations), and the biased state prediction is obtained, taking into account the associated weights for each sigma point [20]. The state prediction is biased, since the unknown inputs are not taken into account:

$$\chi_k^{b(l)} = f\left(\chi_{k-1}^{(l)}, u_{k-1} \right) \tag{4}$$

$$\hat{x}_k^b = \sum_{l=0}^{2n} W^{(l)} \chi_k^{b(l)} \tag{5}$$

where

$$\begin{aligned} W^{(0)} &= \frac{\kappa}{n+\kappa} \\ W^{(l)} &= \frac{1}{2(n+\kappa)}, \qquad l = 1, 2, ..., 2n \end{aligned} \tag{6}$$

3) Biased state error covariance calculation:

$$P_k^b = \sum_{l=0}^{2n} W^{(l)} \left(\chi_k^{b(l)} - \hat{x}_k^b \right) \left(\chi_k^{b(l)} - \hat{x}_k^b \right)^T \tag{7}$$

4) Biased measurement prediction: Here, the sigma points are instantiated through the measurement model, so as to obtain the biased predicted measurements ($\hat{y}_k^b$):

$$\gamma_k^{b(l)} = h\left(\chi_k^{b(l)}, u_k \right) \tag{8}$$

$$\hat{y}_k^b = \sum_{l=0}^{2n} W^{(l)} \gamma_k^{b(l)} \tag{9}$$

5) Calculation of the biased cross-covariance between the states and the predicted measurements:

$$P_{xyk}^{b} = \sum_{l=0}^{2n} W^{(l)} \left(\chi_k^{b(l)} - \hat{x}_k^b\right)\left(\gamma_k^{b(l)} - \hat{y}_k^b\right)^T \tag{10}$$

B. Unknown Input Estimation

As previously stated, the unknown input estimation procedure is very similar to the ones in [14], [15], but, in those cases, a linear relationship was assumed between the states and the measurements. To address the nonlinear measurement function case, Jacobian based linearisation could be one option, but this would defeat the purpose of the derivative-free sigma point based method utilization. Therefore, the statistical linearisation approach is used [19], [21]. This relies on the following concept: The sigma points are instantiated through the measurement model, and the two sets of sigma points (i.e the ones corresponding to the dynamic state - $\chi_k^{b(l)}$ - and the ones corresponding to the predicted measurement - $\gamma_k^{b(l)}$) are used so as to formulate a least square linear regression problem, in order to find a linear approximation of the nonlinear measurement function [19], [21]:

$$\begin{aligned} h(x_k) &\approx H_{mk}x_k + c_k + e_k \\ H_{mk} &= (P_{xyk}^b)^T (P_k^b)^{-1} \\ c_k &= \hat{y}_k^b - H_{mk}\hat{x}_k^b \end{aligned} \tag{11}$$

where e_k is a zero mean random variable. Therefore, the unknown input vector can be estimated through a linear regression model, as shown below [14]:

$$\tilde{y}_k = y_k - \hat{y}_k^b = H_{mk}Gd_{k-1} + \Delta_k \tag{12}$$

where

$$\begin{aligned} \Delta_k &= H_{mk}\left(f\left(x_{k-1}, u_{k-1}, w_{k-1}\right) - \hat{x}_k^b\right) + \upsilon_k \\ E(\Delta_k) &= 0 \\ E(\Delta_k\Delta_k^T) &= H_{mk}P_k^bH_{mk}^T + R_k = \tilde{R}_k \end{aligned} \tag{13}$$

Thus, the unknown input vector is calculated through weighted least squares, to obtain the unbiased estimate [22]:

$$\hat{d}_{k-1} = \left(G^TH_{mk}^T\tilde{R}_k^{-1}H_{mk}G\right)^{-1}G^TH_{mk}^T\tilde{R}_k^{-1}\tilde{y}_k \tag{14}$$

The unknown input estimation equation above requires that $rank(H_{mk}G) = rank(G) = m$, meaning that the number of measurement outputs (m) has to be at least equal to the number of unknown inputs (p), in contrast to [9], where, in the mentioned method, the number of measurement outputs has to necessarily be greater than the number of unknown inputs.

C. Unbiased State Estimation

Since the unknown inputs have been estimated, the standard UKF procedure can be followed, so as to obtain the state estimates. The formerly unknown inputs are now known and they are considered as normal inputs. The UKF algorithm can be summarized as follows:

1) Unbiased (a priori) state prediction:

$$\chi_k^{u(l)} = f\left(\chi_{k-1}^{(l)}, u_{k-1}\right) + G\hat{d}_{k-1} \tag{15}$$

$$\hat{x}_k^{u-} = \sum_{l=0}^{2n} W^{(l)}\chi_k^{u(l)} \tag{16}$$

2) Unbiased a priori state error covariance calculation:

$$P_k^{u-} = \sum_{l=0}^{2n} W^{(l)}\left(\chi_k^{u(l)} - \hat{x}_k^{u-}\right)\left(\chi_k^{u(l)} - \hat{x}_k^{u-}\right)^T \tag{17}$$

3) Unbiased measurement prediction:

$$\gamma_k^{u(l)} = h\left(\chi_k^{u(l)}, u_k\right) \tag{18}$$

$$\hat{y}_k^u = \sum_{l=0}^{2n} W^{(l)}\gamma_k^{u(l)} \tag{19}$$

4) Unbiased predicted measurement covariance estimation:

$$P_{yk}^u = \sum_{l=0}^{2n} W^{(l)}\left(\gamma_k^{u(l)} - \hat{y}_k^u\right)\left(\gamma_k^{u(l)} - \hat{y}_k^u\right)^T + R_k \tag{20}$$

5) Calculation of the unbiased cross-covariance between the states and the predicted measurements:

$$P_{xyk}^u = \sum_{l=0}^{2n} W^{(l)}\left(\chi_k^{u(l)} - \hat{x}_k^{u-}\right)\left(\gamma_k^{u(l)} - \hat{y}_k^u\right)^T \tag{21}$$

6) Measurement update of the state estimate (or a posteriori state estimate):

$$K_k = P_{xyk}^u\left(P_{yk}^u\right)^{-1} \tag{22}$$

$$\hat{x}_k^{u+} = \hat{x}_k^{u-} + K_k\left(y_k - \hat{y}_k^u\right) \tag{23}$$

$$P_k^{u+} = P_k^{u-} - K_kP_{yk}^uK_k^T \tag{24}$$

The steps (3)-(24) constitute the proposed UKF based algorithm for dynamic state and unknown input estimation in the context of power systems, henceforth termed as UKF-UI method. All these calculations are repeated at every time step.

D. Remarks

1) Different set of sigma points: Apart from the aforementioned set of sigma points, several variants have also been proposed in literature [12]. When κ=0, this results in 2n sigma points (instead of 2n+1 of the standard UKF case, since the estimate $\hat{x}_{k-1}^{u+}$ is no longer regarded as part of the sigma points). This corresponds to the Cubature Kalman filter (CKF), whose algorithm coincides with the UKF one, using the set of sigma points as defined below [23], [24]:

$$\begin{aligned} \chi_{k-1}^{(l)} &= \left[\hat{x}_{k-1}^{u+} + \tilde{x}^{(l)}\right], \qquad l = 1, 2, ..., 2n \\ \tilde{x}^{(l)} &= \left(\sqrt{nP_{k-1}^{u+}}\right)_l, \qquad l = 1, 2, ..., n \\ \tilde{x}^{(n+l)} &= -\left(\sqrt{nP_{k-1}^{u+}}\right)_l, \qquad l = 1, 2, ..., n \end{aligned} \tag{25}$$

Substituting $\kappa = 0$ in Eqs. (4)-(24), the algorithm for joint dynamic state and unknown input estimation will be henceforth termed as CKF-UI method, to distinguish from the aforementioned UKF-UI algorithm.

2) Augmented state: The system equations (1) are formulated in such a way so as to accommodate cases when there is nonlinear process noise driving the system. In general, process noise accounts for the mismatch between the true generator model, and the inferred one which is used for estimation purposes. Process noise is associated with numerical integration errors, modelling uncertainty, and noise of measurements which are used as inputs, driving the dynamic system [12], [25], [26]. It can be additive or nonlinear, depending on what it represents. Additive process noise usually accounts for modelling uncertainty and numerical integration errors, whereas nonlinear process noise is often associated with noise coming from measured inputs, which have a nonlinear relationship with the dynamic states [12], [26]. Nonlinear process noise is handled by augmenting the state vector with the nonlinear noise terms [7], [12], [20]:

$$\boldsymbol{x} = \begin{bmatrix} x \\ w_p \end{bmatrix} \tag{26}$$

In this case, the augmented state error covariance has the following form [7], [12], [20]:

$$\boldsymbol{P} = \begin{bmatrix} P_x & P_{w_p x}^T \\ P_{w_p x} & P_{w_p} \end{bmatrix} \tag{27}$$

where P_x is the state error covariance, and $P_{w_p x}$ is the cross-correlation between the states and the nonlinear process noise terms. The nonlinear process noise covariance (P_{w_p}) is considered to be constant, equal to Q_p. It has to be noted that the vectors and matrices in bold associated with the augmented state vector $\boldsymbol{x}$. It has to be noted that, although the state vector can be further augmented in order to include the additive process noise terms [12], this approach is not followed here, for two reasons: First, to avoid dealing with large covariance matrices, which could negatively contribute to the computational time. Secondly, in this way, the additive process noise is not included in the statistical linearisation procedure, so as for the linearisation error not to encompass its effect, resulting in better approximation of the measurement function [19], [27]. Therefore, the additive process noise covariance matrix has to be added to the state covariance matrices related to additive process noise, after the statistical linearisation procedure [19].

III. Synchronous Generator Model

A. Model Development

Synchronous generators constitute the core of a power system. Depending on each study's targets and the modelling detail, various models have been reported in literature [28], [29]. The decentralization procedure is based on system partitioning (in the context of the estimation calculations) and requires some measurements on the assumed 'boundary' to be treated as inputs [7], [30]. There are several approaches in terms of which measurements to be used as inputs, and whether these measurements, which are corrupted with noise, are decoupled [7], [31] or not [6], [9], [32] with their associated noise term. In addition, different models have been utilized to represent the synchronous generator and its associated equations [6], [7], [9], [31], [32]. Here, the synchronous generator subtransient model is used for the UKF-UI/CKF-UI algorithm and it is described by the following equations [17], [28]:

$$\dot{\alpha} = \omega_B \left(\omega - 1 - f_\theta\right) \tag{28}$$

$$\dot{\omega} = \frac{1}{M}\left[T_m - T_e - D\left(\omega - 1\right)\right] \tag{29}$$

where α is the generator's internal voltage angle with respect to the terminal voltage phasor, ω is the p.u. rotor speed, ω_B is the base value for ω, f_θ is the rate of change of the angle of the terminal voltage phasor, M is the inertia characterizing the rotor's mass, T_m is the mechanical torque, coming from the turbine driving the generator, T_e is the electrical torque, associated with the power which the generator is required (by the network) to supply, and D is the damping coefficient, to smoothen ω oscillations in transient conditions. These equations (called 'swing' equations) are important from the stability point of view. ω is conceptually tied with power system frequency [33], and any changes in the power network are reflected on f_θ, driving changes on T_e. The generator's rotor includes coils and flux to produce voltage in the stator, given by the following equations:

$$\begin{aligned}\dot{E}'_q = \frac{1}{T'_{d0}}\Big\{E_{fd} - E'_q - \left(X_d - X'_d\right)\Big[-I_d \\ - \frac{K_{d2}}{X'_d - X_{ls}}\left(\psi_{1d} - \left(X'_d - X_{ls}\right)I_d - E'_q\right)\Big]\Big\}\end{aligned} \tag{30}$$

$$\begin{aligned}\dot{E}'_d = \frac{1}{T'_{q0}}\Big\{-E'_d - \left(X_q - X'_q\right)\Big[I_q \\ - \frac{K_{q2}}{X'_q - X_{ls}}\left(-\psi_{2q} + \left(X'_q - X_{ls}\right)I_q - E'_d\right)\Big]\Big\}\end{aligned} \tag{31}$$

$$\dot{\psi}_{2q} = \frac{1}{T''_{q0}}\left[-\psi_{2q} - E'_d + \left(X'_q - X_{ls}\right)I_q\right] \tag{32}$$

$$\dot{\psi}_{1d} = \frac{1}{T''_{d0}}\left[-\psi_{1d} + E'_q + \left(X'_d - X_{ls}\right)I_d\right] \tag{33}$$

and

$$\begin{aligned}T_e = K_{q1}E'_d I_d + K_{d1}E'_q I_q \\ + \left(X''_d - X''_q\right)I_d I_q + K_{d2}\psi_{1d}I_q - K_{q2}\psi_{2q}I_d\end{aligned} \tag{34}$$

$$\begin{bmatrix} I_d \\ I_q \end{bmatrix} = \begin{bmatrix} R_s & X''_q \\ -X''_d & R_s \end{bmatrix}^{-1}\begin{bmatrix} K_{q1}E'_d - K_{q2}\psi_{2q} - V_d \\ K_{d1}E'_q + K_{d2}\psi_{1d} - V_q \end{bmatrix} \tag{35}$$

$$V_q = V cos\alpha \tag{36}$$

$$V_d = -V sin\alpha \tag{37}$$

$$V = V_y - V_v \tag{38}$$

$$f_\theta = f_y - f_v \tag{39}$$

All these equations formulate the subtransient generator model, which has been thoroughly analysed in literature (for instance [17], [28], [29]). The equations have been given in continuous form, but they can be discretized assuming that $\dot{x} = (x_k - x_{k-1})/T_0$, where T_0 is the simulation time step. This model is built based on the principle that d-axis leads q-axis. It can be noticed that the rotor angle (δ) is not part of

the state variable used here, but the internal rotor angle (α) is utilized instead. The notion behind this choice is that, in a multi-machine power system model, the rotor angle (δ_i) and the stator voltage phase (θ_i) of each generator i, which are significant for the generator's internal parameters, are defined with respect to a common reference frame. However, in the context of decentralization, the knowledge of the values of these quantities would require knowledge of the common reference frame, which would defeat the purpose of decentralization [31]. To handle this, we can use the internal rotor angle as a state variable, as carried out in [9], but defined as $\alpha = \delta - \theta$ and employing Eq. (28) to describe its dynamics [31]. The rate of change of the stator voltage phase can be approximated by the equation below (here divided by ω_B, to obtain the p.u. value) [28]:

$$f_{\theta k} \approx \frac{\theta_k - \theta_{k-1}}{\omega_B T_0} \tag{40}$$

Assuming that in the beginning of the simulation the system is in steady state operation, the initial internal rotor angle value can be given by the following equation (with '0' subscripts denoting initial conditions) [34]:

$$\alpha_0 = arctan\left(\frac{X_q I_0 cos\phi_0 + R_s I_0 sin\phi_0}{V_0 + X_q I_0 sin\phi_0 - R_s I_0 cos\phi_0}\right) \tag{41}$$

Following the procedure described in [31], the measurements of the stator voltage magnitude (V_y) and the rate of change of its phase (f_y) are considered as inputs, whereas their noise terms (V_υ and f_υ) are regarded as part of the augmented state vector [7]. This means that the measurement noise of these quantities are considered as '*pseudo process noise*' (using the same terminology as in [7]), showing that this form of nonlinear noise is assumed to drive the estimation model here. Additionally, process noise, representing consideration of modelling uncertainty, is added to each state variable. Therefore, the synchronous machine state-space model includes the state vector as follows:

$$x_a = \left[\alpha\ \omega\ E'_q\ E'_d\ \psi_{2q}\ \psi_{1d}\ V_\upsilon\ f_\upsilon\right]^T \tag{42}$$

Also, the input vector is:

$$u = \left[V_y\ f_y\right]^T \tag{43}$$

Whereas the unknown input vector is:

$$d = \left[T_m\ E_{fd}\right]^T \tag{44}$$

The unknown input distribution matrix is given by:

$$G = \begin{bmatrix} 0 & \frac{T_0}{M} & 0 & 0 & 0 & 0 & 0 & 0 \\ 0 & 0 & \frac{T_0}{T'_{d0}} & 0 & 0 & 0 & 0 & 0 \end{bmatrix}^T \tag{45}$$

The nonlinear relationship between the states is clear from the Eqs. (28 - 39).

Given the presence of both additive and nonlinear process noise in our generator estimation model, in the context of the discussion in Section II-D regarding the consideration of an augmented state vector, the following additive process noise covariance matrix is added to the additive process noise related state covariance matrices, in Eqs. (14), (17):

$$\boldsymbol{Q} = \begin{bmatrix} Q & \mathbf{0}_{6\times 2} \\ \mathbf{0}_{2\times 6} & \mathbf{0}_{2\times 2} \end{bmatrix} \tag{46}$$

The proposed UKF-UI/CKF-UI (depending on the set of sigma points used) algorithm, for the generator estimation model used here, is summarized in Appendix A.

B. Rank requirement and measurement quantities selection

Following the practice in [7], [31], the stator current measured magnitude (I_y) and its measured phase with reference to the voltage phasor (ϕ_{Iy}) are the measurements which are treated as system outputs. These are given by the following equations:

$$I_y = \sqrt{I_q^2 + I_d^2} + \upsilon_I \tag{47}$$

$$\phi_{Iy} = \alpha + arctan\left(\frac{I_d}{I_q}\right) + \upsilon_{\phi_I} \tag{48}$$

and I_q, I_d are given by Eq. (35), whereas υ_I, υ_{ϕ_I} are the measurement noise terms, associated with I_y and ϕ_{Iy}, respectively.

However, careful attention has to be paid to the rank requirement of the unknown input estimation procedure, according to which $rank(H_m G) = m$. With regard to Eq. (14), in mathematical terms, this means that, the matrix inversion which is involved in this equation is not possible when the rank requirement is violated, due to singularity which arises, and the unknown input estimation is impossible. In practical terms, this is closely related to the measurement variables chosen as system outputs. More specifically, given matrices G, x and d, the unknown inputs are reflected on ω and E'_q. In turn, the rank requirement of $H_m G$ is violated when at least one of columns 2, 3 of matrix H_m is a column of zeros, since this would result in a column of zeros in $H_m G$. Given the state vector x, columns 2, 3 of matrix H_m correspond to ω and E'_q, respectively. This means that these two states have to be able to be viewed from the measurements/outputs. Using just I and ϕ_I as outputs, given Eqs. (47, 48, 35), it is clear that ω is not reflected on the measurements. Therefore, frequency measurement (f_{sys_y}) has also been considered, since it is closely related to speed [33], and its p.u. value is:

$$f_{sys_y} = \omega + \upsilon_f \tag{49}$$

where υ_f is the associated measurement noise. This is the reason why frequency measurement is considered in [9] as well. Thus, the measurement vector is the following:

$$y = \left[f_{sys_y}\ I_y\ \phi_{Iy}\right]^T \tag{50}$$

C. Model Initialization

The synchronous generator model is initialized assuming that the system operates in steady state. Since the terminal voltage and current magnitudes, along with their phase difference, can be obtained from the PMU at the terminal bus [9],

and the global reference frame is unknown, the reference frame is considered to coincide with the position of the terminal voltage phasor. Therefore, if $\boldsymbol{V}_0 = V^{\angle 0}$ and $\boldsymbol{I}_0 = I_0^{\angle -\phi_0}$, the initial conditions of all states and unknown inputs can be derived from the following equations (with subscripts '0' denoting initial conditions) [35]:

$$E_{q0}^{\angle \alpha_0} = V_0^{\angle 0} + (R_s + jX_q)\, I_0^{\angle -\phi_0} \tag{51}$$

$$I_{d0} = -I_0 sin\,(\alpha_0 - (-\phi_0)) \tag{52}$$

$$I_{q0} = I_0 cos\,(\alpha_0 - (-\phi_0)) \tag{53}$$

$$V_{d0} = -V_0 sin\,(\alpha_0) \tag{54}$$

$$V_{q0} = V_0 cos\,(\alpha_0) \tag{55}$$

$$E_{fd0} = E_{q0} - (X_d - X_q)\, I_{d0} \tag{56}$$

$$E'_{q0} = E_{fd0} + (X_d - X'_d)\, I_{d0} \tag{57}$$

$$E'_{d0} = -\left(X_q - X'_q\right) I_{q0} \tag{58}$$

$$\psi_{2q0} = -E'_{d0} + \left(X'_q - X_{ls}\right) I_{q0} \tag{59}$$

$$\psi_{1d0} = E'_{q0} + (X'_d - X_{ls})\, I_{d0} \tag{60}$$

$$T_{m0} = T_{e0} \tag{61}$$

and T_{e0} is given by Eq. (34).

IV. Case Studies

The UKF-UI/CKF-UI algorithm has been implemented in a 68-bus 16-machine system model, shown in Fig. 1, the details of which can be found in [18]. It has to be highlighted that, in this model, the synchronous generator subtransient model is used for all the machines, and, therefore, the synchronous generator is characterized by the subtransient model for the purpose of estimation. However, in the context of power system model, an additional state variable is used as part of the synchronous generator model, the transient emf (E'_{dc}) due to flux linkage of a dummy coil in the q-axis [35]. But, this is utilized to facilitate the multi-machine system simulation [35], thus it is not needed in the synchronous machine decentralized model for UKF-UI/CKF-UI. Power system modelling is MATLAB/Simulink based, and all simulations continue for 10 s. Measurements are obtained by PMUs having reporting rate of 120 frames per second, according to IEEE Standards [36], [37]. The standard deviation concerning the process and measurement noise is assumed to be 10^{-6}. Two case studies have been considered:

- *Case Study 1A:* A three-phase to ground fault occurs at bus 25 at the time instant $t = 2$ s, it is cleared after 100 ms and the line connecting buses 25 and 26 is tripped at the same time.
- *Case Study 1B:* A step increase by 1 p.u. in T_m of Gen. 5 occurs at the time instant $t = 2$ s and lasts for 1 s, returning to its previous value afterwards.

As previously stated, an EKF based state estimation method for power systems with unknown inputs has been recently proposed (termed as EKF-UI) [6], [9]. Thus, it would be interesting to assess the performance of that method and the ones developed here (i.e. UKF-UI and CKF-UI) in the context of the aforementioned case studies. The main differences between UKF-UI/CKF-UI and EKF-UI can be summarized as follows:

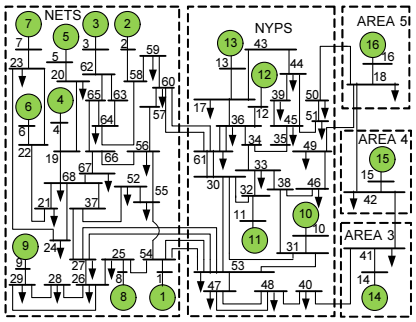

Fig. 1: NETS-NYPS 68-bus, 16-machine system

- In order to apply EFK-UI, the Jacobians for state and measurement equations have to be calculated. This procedure is not needed in UKF-UI/CKF-UI;
- In UKF-UI/CKF-UI, the unknown inputs are calculated at every time step, based on a linear regression model as explained earlier, without any relationship to arise between their values at two successive time steps. In EKF-UI, the estimation procedure is based on a different approach, where the unknown input estimation is based on a formula dependent on the unknown input's estimated value of the previous time step [6], [9];
- In EFK-UI, the number of measurements has to be greater than the number of unknown inputs at every time step [6], [9], whereas in UKF-UI, the number of measurement is required to be at least equal to the number of unknown inputs.

Therefore, here, all techniques are utilized, based on the same measurements and models developed in the context of this research effort and analysed in earlier sections, so as to evaluate all estimation algorithms under the same conditions and assumptions.

As far as the case study 1A is concerned, the state and unknown input estimation results are illustrated in Figs 2, 3 regarding Gen. 8. In addition, the state and unknown input estimation results are depicted in Figs. 4, 5 for the case study 1B concerning Gen. 5. The effectiveness of UKF-UI and CKF-UI methods can be clearly noticed, as all algorithms are reveal highly accurate results.

V. Robustness Assessment

A. Sensitivity to parameter errors

Uncertainty is present in power system operation, and system operators are likely to consider erroneous data in power system analysis, due to various reasons, such as ageing components [1]. Therefore, it is interesting to assess the performance of UKF-UI and CKF-UI methods, when there is 10% error in X_q and X'_q of the generator studied in each case study. Here, case study 1A has been revisited, and the results for Gen. 8 are illustrated in Figs. 6 and 7. It can be noticed that the estimation model dynamics are excited to a small extent before the contingency occurrence, reflecting the incorrect system initialization considering the erroneous parameters. Also, unknown input estimation results are accurate towards the end of the transient period, whereas state estimation results

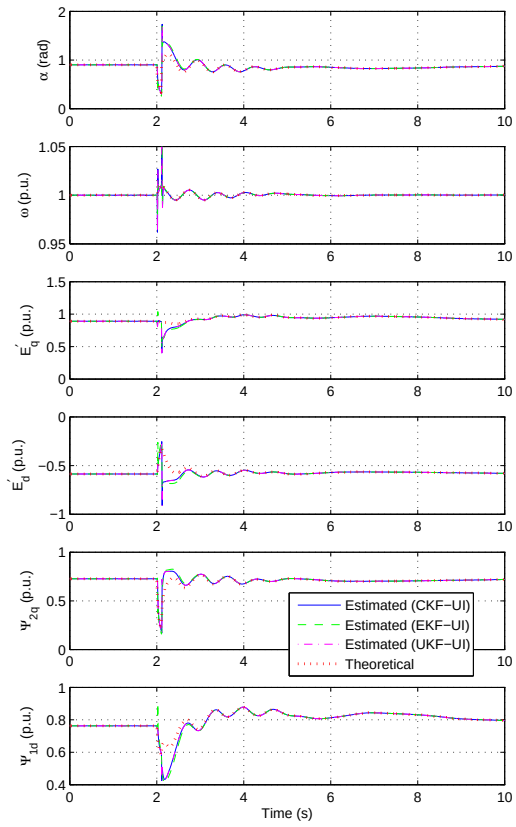

Fig. 2: Case Study 1A: Dynamic state estimation of Gen. 8

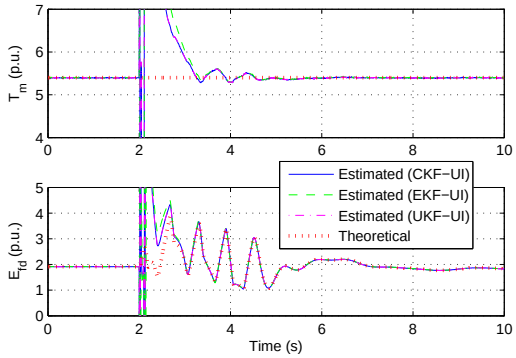

Fig. 3: Case Study 1A: Unknown input estimation of Gen. 8

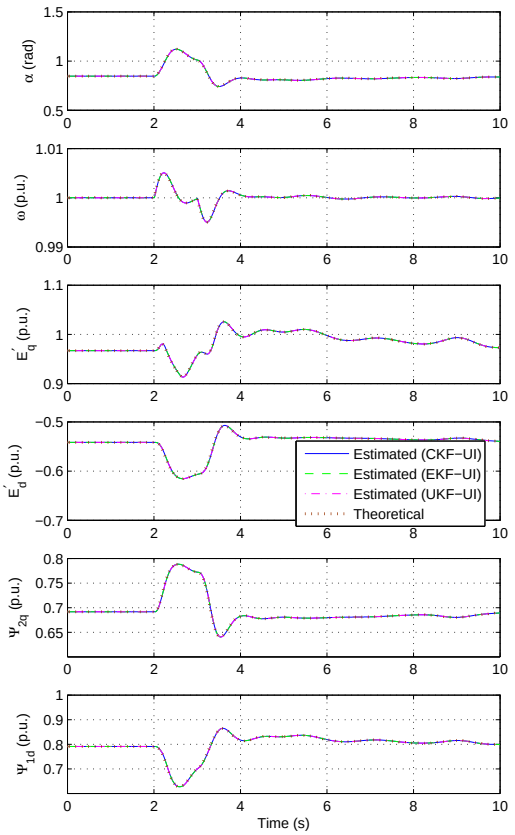

Fig. 4: Case Study 1B: Dynamic state estimation of Gen. 5

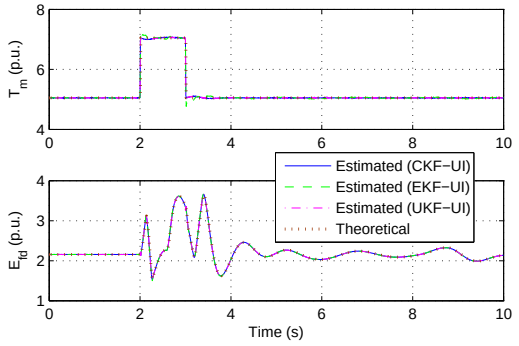

Fig. 5: Case Study 1B: Unknown input estimation of Gen. 5

are characterized by a small steady state error apart from rotor speed, which is highly viewable through system frequency measurements. Similar observations have been noted in [9], under similar sensitivity analysis. Therefore, good knowledge of the local machine parameters under study is required to achieve highly accurate estimation results.

B. Sensitivity to process and measurement noise

As discussed in Section II-D, process noise is associated with model integration errors, model uncertainty and noise coming from measured inputs. The success of the UKF-UI/CKF-UI algorithm has been validated in the previous case studies, but these are based on the assumptions that system modelling approximations are low and PMUs give highly accurate measurements. However, in practice the measurement noise can be higher. According to the IEEE Standard C37.118.1-2011 and its recent amendment C37.118.1a-2014, the basic time synchronisation accuracy is 0.2 μs [11], [36], [37], which corresponds to phase measurement error of ± 0.08 mrad, for a 60-Hz system. Also, the frequency error has to be up to 0.005 Hz [36], [37]. Furthermore, the current and voltage magnitude measurements are limited by the accuracy of the instrument transformers [38], and the IEEE Standard C57.13-2008 specifies the instrument transformers' accuracy within the range of 0.1% and 0.3% [11], [39].

Taking these into account, the estimation procedure has been re-examined against high process noise levels. This consists of high measurement noise levels for the measured inputs (i.e. standard deviation of 10^{-3} p.u. for voltage and 0.08 mrad for

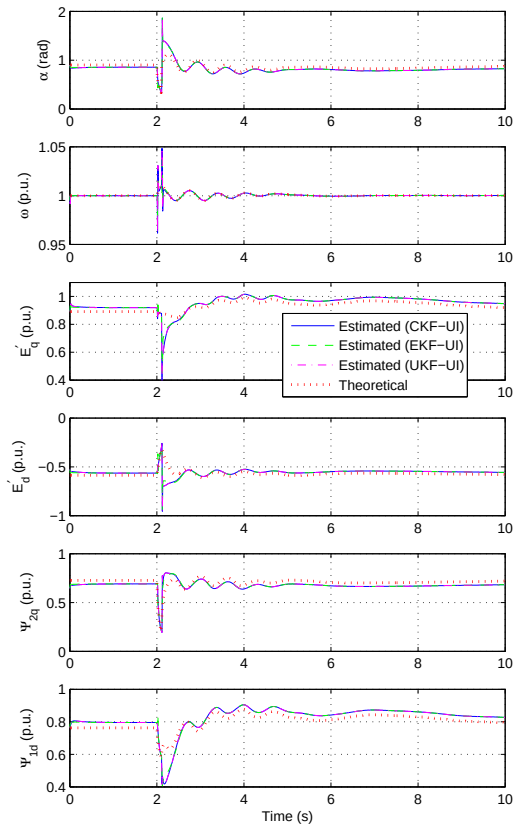

Fig. 6: Case Study 1A: Dynamic state estimation in the presence of 10% error in X_q and X_q' of Gen. 8

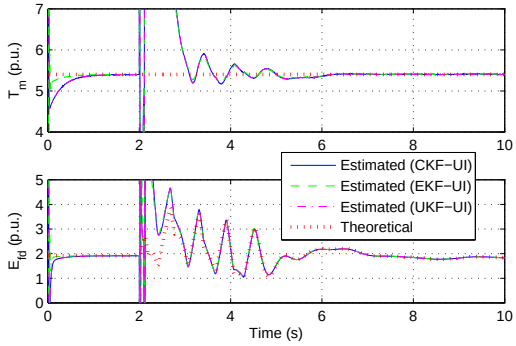

Fig. 7: Case Study 1A: Unknown input estimation in the presence of 10% error in X_q and X_q' of Gen. 8

its phase), which correspond to nonlinear process noise, as well as high levels of additive process noise, corresponding to standard deviation of 10^{-3} for all states, in a similar approach followed in [25], accounting for 10% of the largest state changes in one time step. High value of additive noise covariance Q means that 'fictitious' noise is added to the estimation model, so as for the filter to include a larger emphasis on the measurement correction part, which is important when unmodelled dynamics are present, as explained in [12]. The results for the previous case studies are shown in Figs. 8, 9 for the case study 1A and Gen. 8, and in Figs. 10, 11 for the case study 1B and Gen. 5. The robustness of the proposed methods is evidently showcased with respect to the dynamic state estimation, whereas the unknown input estimation is greatly affected by the high process noise levels. This is due to the fact that the UKF-UI/CKF-UI algorithm is optimized for the estimation of the dynamic states, whose behaviour is described by known equations. Similar performance has been observed for EKF-UI.

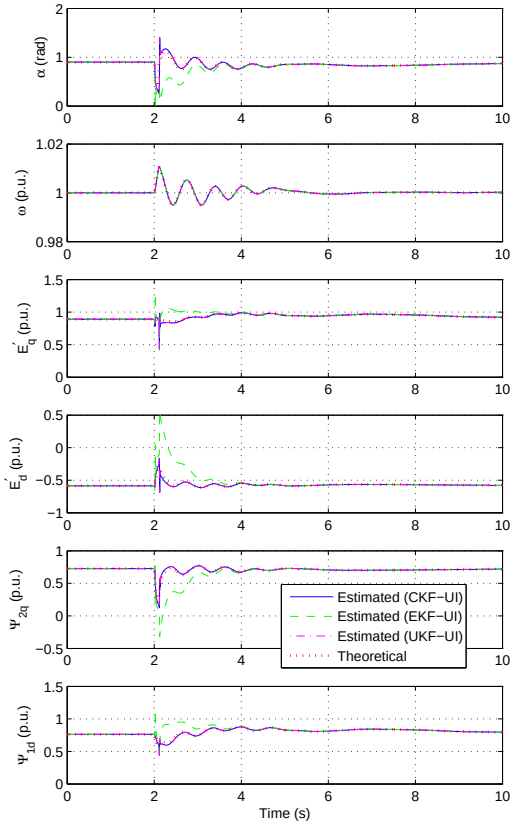

Fig. 8: Case Study 1A: Dynamic state estimation of Gen. 8 under high process noise levels

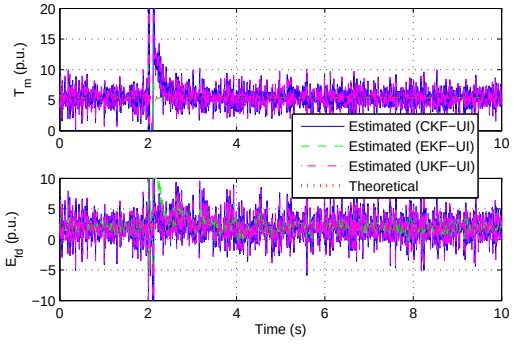

Fig. 9: Case Study 1A: Unknown input estimation of Gen. 8 under high process noise levels

The proposed algorithm has also been tested against high measurement noise levels for the measurements obtained (i.e. the ones forming the measurement vector y), considering low process noise levels. The results are illustrated in Figs. 12, 13 for the case study 1A and Gen. 8, and in Figs. 14, 15 for the case study 1B and Gen. 5. It can be observed that they are similar to the ones with high process noise levels,

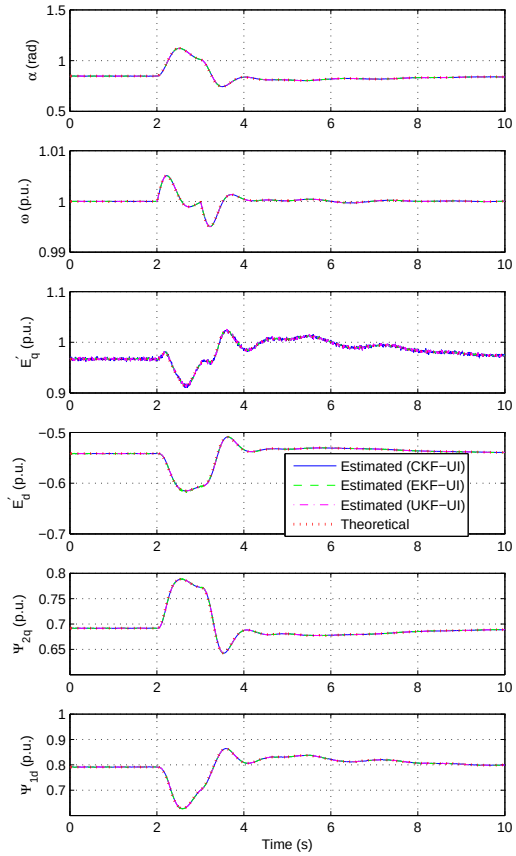

Fig. 10: Case Study 1B: Dynamic state estimation of Gen. 5 under high process noise levels

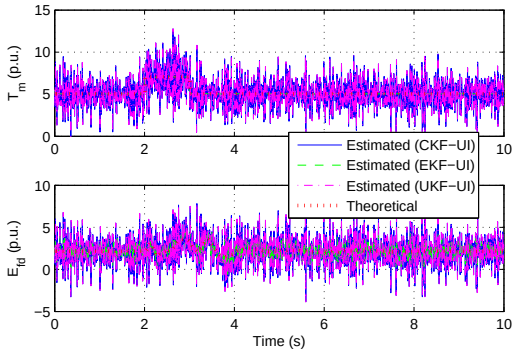

Fig. 11: Case Study 1B: Unknown input estimation of Gen. 5 under high process noise levels

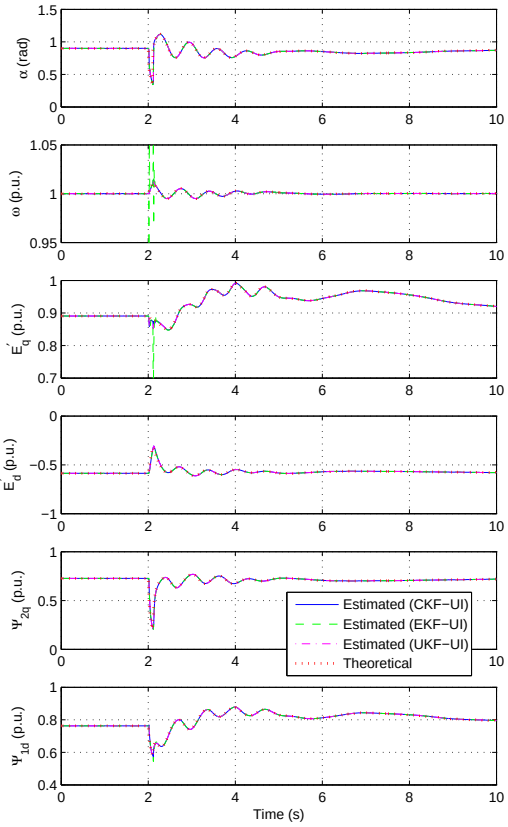

Fig. 12: Case Study 1A: Dynamic state estimation of Gen. 8 under high measurement noise levels

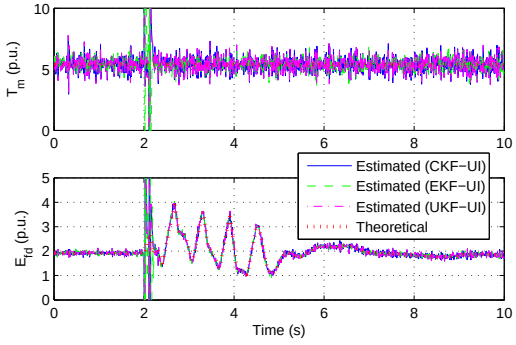

Fig. 13: Case Study 1A: Unknown input estimation of Gen. 8 under high measurement noise levels

meaning that the dynamic state estimates are highly accurate, as opposed to the unknown input estimates, showing higher sensitivity to measurement noise increase.

Since highly noisy measurements affect the unknown input estimation performance from both process and measurement noise related points of view, it is required to search for noise impact mitigation strategies. This has been done in two ways: Finding ways of obtaining more accurate measurements, and increasing the number of measurable quantities in our model.

1) Discussion on measurement noise reduction: Noise reduction has been thoroughly tackled in the context of other fields, such as signal processing. As far as power systems are concerned, the advent of PMUs and their significance in wide area monitoring has triggered research studies on measurement noise mitigation. Various techniques have been reported in literature, such as:

- Empirical mode decomposition (EMD) methods [40], [41];
- Singular value decomposition (SVD) based algorithms [42];
- Wavelet shrinkage procedures [40], [43], [44];
- Integrated calibration techniques [45], [46];
- Multiple measurement averaging processes (also termed as 'data buffering') [47], [48].

However, these methods mainly aim at offline denoising.

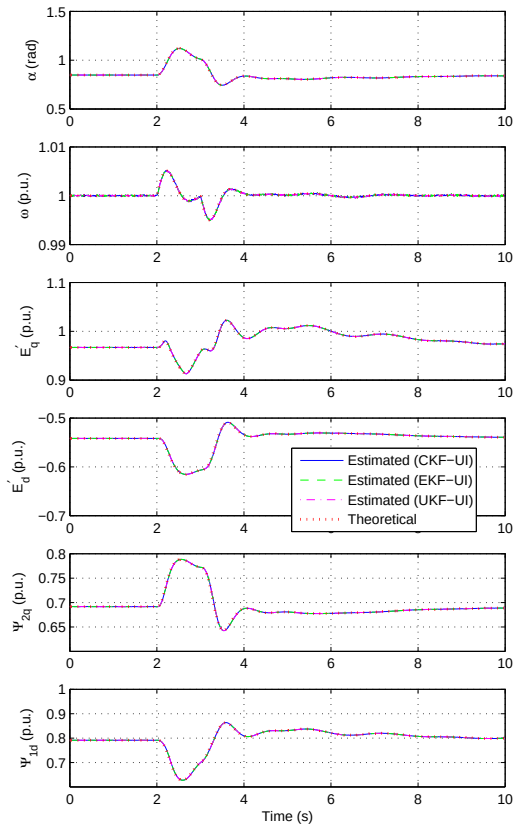

Fig. 14: Case Study 1B: Dynamic state estimation of Gen. 5 under high measurement noise levels

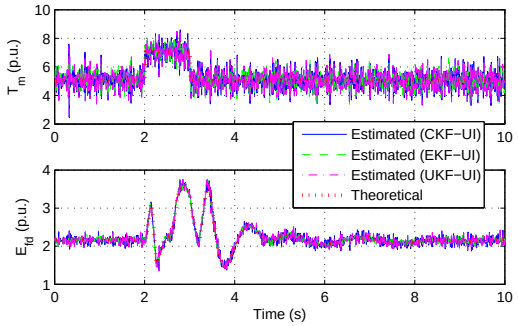

Fig. 15: Case Study 1B: Unknown input estimation of Gen. 5 under high measurement noise levels

Real-time denoising's importance has been recently highlighted in power systems [40]. Online measurement noise reduction algorithms include Kalman filtering based approaches [49], and methods including autoregressive models, which has been reported in the field of real-time glucose monitoring [50]. Furthermore, novel algorithms, integrated within PMUs' software have the capability to report measurements with increased accuracy [51]–[55]. In addition, PMU algorithms have been employed so as to minimize their execution time, enabling the existence of PMUs with reporting rates as high as 5000 frames per second [56]. This capability can be found useful in the context of data buffering as well.

2) Consideration of additional measurements: Attempting to enhance the unknown input estimation accuracy, additional measurements can facilitate this purpose [9]. This depends on the decentralized model used, in terms of the measurable quantities, and the model used here enables the use of more quantities as measurements (in contrast with the model in [9], for instance). PMUs have the capability of measuring active and reactive power [9], thus, the previous case studies have been re-examined, considering these additional measurements, since this can be accomplished through the decentralized model used here. The measurement functions for these are given as follows:

$$P_y = K_{q1}E'_dI_d + K_{d1}E'_qI_q + \left(X''_d - X''_q\right)I_dI_q + K_{d2}\psi_{1d}I_q - K_{q2}\psi_{2q}I_d - \left(I_d^2 + I_q^2\right)R_s + \upsilon_P \quad (62)$$

$$Q_y = K_{q1}E'_dI_q - K_{q2}\psi_{2q}I_q - X''_qI_q^2 - X''_dI_d^2 - K_{d1}E'_qI_d - K_{d2}\psi_{1d}I_d + \upsilon_Q \quad (63)$$

where P_y and Q_y are the active and reactive power, respectively, measured at the generator's terminal bus. The measurement vector is then the following one:

$$y = \left[f_{sys_y}\ I_y\ \phi_{Iy}\ P_y\ Q_y\right]^T \quad (64)$$

Here, considering the worst case scenario, same high process and measurement noise levels as earlier are considered, but assuming 1800 Hz PMU reporting rate (in accordance with the research findings listed previously), while the UKF-UI/CKF-UI algorithm runs twice per cycle, and, therefore, 15 measurements of every output are averaged every time that the algorithm iterates. The results are depicted in Figs. 16, 17 for the case study 1A regarding Gen. 8, and in Figs. 18, 19 for the case study 1B concerning Gen. 5. The results are acceptable in terms of unknown input estimation.

VI. Computational feasibility

As previously stated, in all cases the UKF-UI/CKF-UI algorithm runs twice per cycle, in the context of a 60 Hz system. Therefore, the algorithm is repeated at a frequency of 120 Hz. As a result, it is important for the whole procedure to be completed within a shorter time frame than the simulation time step (which is $1/120 \approx 8.33$ ms). It has to be mentioned that this study has been conducted on MATLAB/Simulink, using a personal computer with Intel Xeon E5-1650, 3.20 GHz CPU and 16 GB RAM. The average time required for one iteration for all methods are depicted in Table I. The proposed UKF-UI and CKF-UI appear to require more time to be executed than EKF-UI, which is expected, since they include more equations. CKF-UI is also proven to be faster than UKF-UI, which can be justified by considering that UKF-UI engages one more sigma point for each state, resulting in larger matrices. Most importantly, all methods require less amount of time than 8.33 ms, thus, they can be implemented in real time.

TABLE I: Computational speed assessment

Method	Average execution time for one iteration (ms)
EKF-UI	0.41
CKF-UI	0.54
UKF-UI	0.71

Algorithm: UKF-UI/CFK-UI

The augmented state vector, known inputs, and unknown inputs are given by the vectors in Eqs. (42), (43), and (44), respectively. State equations f are given by the discrete form of Eqs. (28)-(39), whereas measurement equations h are given by Eqs. (49), (47), (48), considering 3 measurements, or Eqs. (49), (47), (48), (62), (63), considering 5 measurements. The length of the augmented state vector is $\boldsymbol{n} = n + 2$.

while $k \geq 1$ **do**

  STEP 1: Initialization

  if $k == 1$ **then**

    Initialize $\hat{x}_0^{u+}$ according to Eqs. (51)-(61), and $\hat{w}_{p0} = \mathbf{0}_{2\times 1}$, therefore $\hat{\boldsymbol{x}}_0^{u+} = [(\hat{x}_0^{u+})^T \quad \mathbf{0}_{2\times 1}^T]^T$.

    Initialize $P_{x0} = Q$, $P_{w_p x0} = \mathbf{0}_{2\times n}$, $P_{w_p 0} = Q_p$, forming $\boldsymbol{P}_0^{u+}$, in accordance with Eq. (27).

  else

    Reinitialize $\hat{w}_{p(k-1)} = \mathbf{0}_{2\times 1}$, and $P_{w_p(k-1)} = Q_p$, while the rest of the elements in $\hat{\boldsymbol{x}}_{k-1}^{u+}$, $\boldsymbol{P}_{k-1}^{u+}$ remain unchanged.

  end if

  STEP 2: Sigma point generation

  Obtain the sigma points from Eq. (3) for UKF-UI, or Eq. (25) for CKF-UI.

  STEP 3: Biased state prediction

  $\boldsymbol{\chi}_k^{b(l)} = f(\boldsymbol{\chi}_{k-1}^{(l)}, u_{k-1})$

  $\hat{\boldsymbol{x}}_k^b = \sum_{l=0}^{2\boldsymbol{n}} W^{(l)} \boldsymbol{\chi}_k^{b(l)}$

  $\boldsymbol{P}_k^b = \sum_{l=0}^{2\boldsymbol{n}} W^{(l)} (\boldsymbol{\chi}_k^{b(l)} - \hat{\boldsymbol{x}}_k^b)(\boldsymbol{\chi}_k^{b(l)} - \hat{\boldsymbol{x}}_k^b)^T$

  STEP 4: Biased measurement prediction

  $\gamma_k^{b(l)} = h(\boldsymbol{\chi}_k^{b(l)}, u_k)$

  $\hat{y}_k^b = \sum_{l=0}^{2\boldsymbol{n}} W^{(l)} \gamma_k^{b(l)}$

  $\boldsymbol{P}_{xyk}^b = \sum_{l=0}^{2\boldsymbol{n}} W^{(l)} (\boldsymbol{\chi}_k^{b(l)} - \hat{\boldsymbol{x}}_k^b)(\gamma_k^{b(l)} - \hat{y}_k^b)^T$

  STEP 5: Unknown input estimation

  $H_{mk} = (\boldsymbol{P}_{xyk}^b)^T (\boldsymbol{P}_k^b)^{-1}$

  $\tilde{R}_k = H_{mk}(\boldsymbol{P}_k^b + \boldsymbol{Q}) H_{mk}^T + R_k$

  $\hat{d}_{k-1} = (G^T H_{mk}^T \tilde{R}_k^{-1} H_{mk} G)^{-1} G^T H_{mk}^T \tilde{R}_k^{-1} (y_k - \hat{y}_k^b)$

  STEP 6: Unbiased state prediction

  $\boldsymbol{\chi}_k^{u(l)} = f(\boldsymbol{\chi}_{k-1}^{(l)}, u_{k-1}) + G\hat{d}_{k-1}$

  $\hat{\boldsymbol{x}}_k^{u-} = \sum_{l=0}^{2\boldsymbol{n}} W^{(l)} \boldsymbol{\chi}_k^{u(l)}$

  $\boldsymbol{P}_k^{u-} = \sum_{l=0}^{2\boldsymbol{n}} W^{(l)} (\boldsymbol{\chi}_k^{u(l)} - \hat{\boldsymbol{x}}_k^{u-})(\boldsymbol{\chi}_k^{u(l)} - \hat{\boldsymbol{x}}_k^{u-})^T + \boldsymbol{Q}$

  STEP 7: Unbiased measurement prediction

  $\gamma_k^{u(l)} = h(\boldsymbol{\chi}_k^{u(l)}, u_k)$

  $\hat{y}_k^u = \sum_{l=0}^{2\boldsymbol{n}} W^{(l)} \gamma_k^{u(l)}$

  $P_{yk}^u = \sum_{l=0}^{2\boldsymbol{n}} W^{(l)} (\gamma_k^{u(l)} - \hat{y}_k^u)(\gamma_k^{u(l)} - \hat{y}_k^u)^T + R_k$

  $\boldsymbol{P}_{xyk}^u = \sum_{l=0}^{2\boldsymbol{n}} W^{(l)} (\boldsymbol{\chi}_k^{u(l)} - \hat{\boldsymbol{x}}_k^{u-})(\gamma_k^{u(l)} - \hat{y}_k^u)^T$

  STEP 8: Kalman update

  $\boldsymbol{K}_k = \boldsymbol{P}_{xyk}^u (P_{yk}^u)^{-1}$

  $\hat{\boldsymbol{x}}_k^{u+} = \hat{\boldsymbol{x}}_k^{u-} + \boldsymbol{K}_k (y_k - \hat{y}_k^u)$

  $\boldsymbol{P}_k^{u+} = \boldsymbol{P}_k^{u-} - \boldsymbol{K}_k P_{yk}^u \boldsymbol{K}_k^T$

  STEP 9: Output and time update

  Output $\hat{\boldsymbol{x}}_k^{u+}$ and $\boldsymbol{P}_k^{u+}$

  $k \longleftarrow (k+1)$

end while

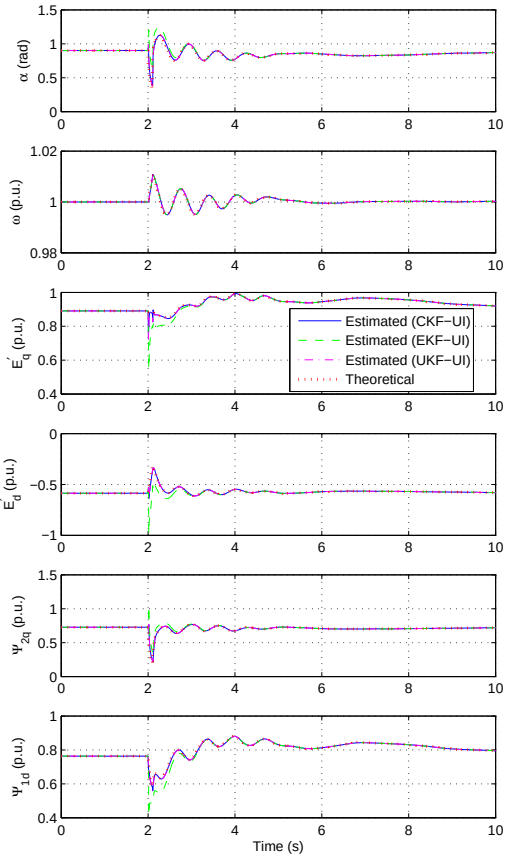

Fig. 16: Case Study 1A: Dynamic state estimation of Gen. 8 under high process and measurement noise levels, using measurement noise impact reduction measures

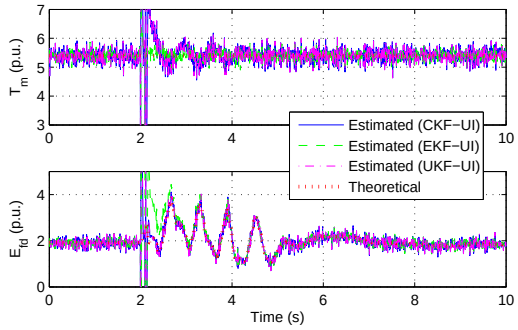

Fig. 17: Case Study 1A: Unknown input estimation of Gen. 8 under high process and measurement noise levels, using measurement noise impact reduction measures

VII. Conclusions

A derivative-free Kalman filtering based decentralized dynamic state estimation algorithm with unknown inputs has been demonstrated, to tackle cases when linearisation is burdensome. The dynamic state estimation process is performed without any prior knowledge or assumptions regarding unknown input models or distributions. The decentralization procedure necessitates voltage magnitude and phase measurements to be treated as inputs, and the consideration of the internal rotor angle as a state variable leads to useful results.

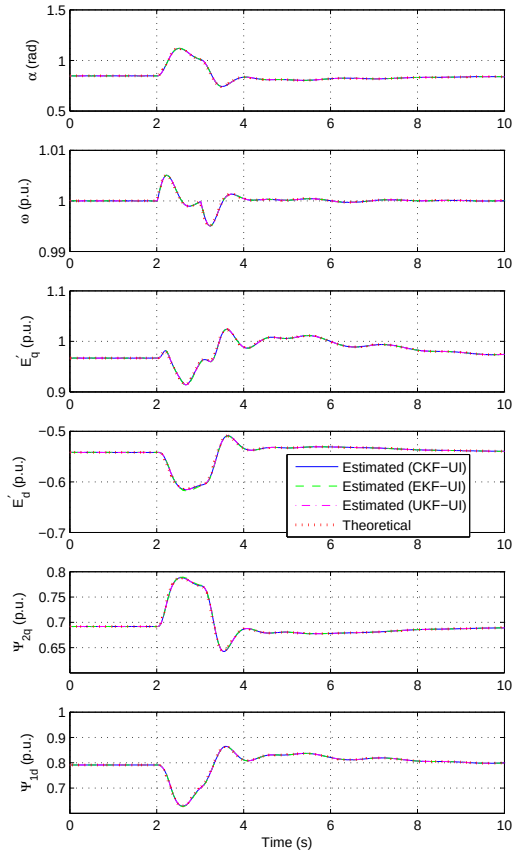

Fig. 18: Case Study 1B: Dynamic state estimation of Gen. 5 under high process and measurement noise levels, using measurement noise impact reduction measures

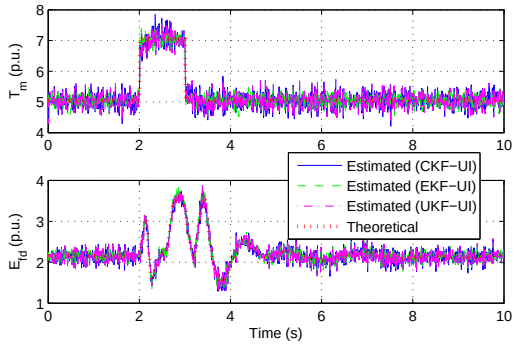

Fig. 19: Case Study 1B: Unknown input estimation of Gen. 5 under high process and measurement noise levels, using measurement noise impact reduction measures

This method has been tested on a realistic large power system model, under low and high process and measurement noise levels, as well as against parameter errors in the estimation model, and it has been proven to be robust. The differences between the proposed methods and an Extended Kalman filtering based decentralized dynamic state estimation approach with unknown inputs have also been highlighted. Measurement noise impact reduction techniques have been proposed in order to further enhance the unknown inputs' estimation accuracy. This suggested methodology constitutes a step forward towards the enhanced accuracy of power system dynamic state estimation, which is significant in terms of stability margin computation and security assessment, in the context of modern power networks, characterised by stochasticity and uncertainty.

APPENDIX A
UKF-UI/CKF-UI ALGORITHM

The UKF-UI/CFK-UI algorithm is presented in a pseudo-code form at the left top of the previous page.

REFERENCES

[1] K. Morison, L. Wang, and P. Kundur, "Power system security assessment," *Power and Energy Magazine, IEEE*, vol. 2, pp. 30–39, Sept 2004.

[2] P. Panciatici, G. Bareux, and L. Wehenkel, "Operating in the Fog: Security Management Under Uncertainty," *Power and Energy Magazine, IEEE*, vol. 10, pp. 40–49, Sept 2012.

[3] C. Taylor, "Improving grid behaviour," *Spectrum, IEEE*, vol. 36, pp. 40–45, Jun 1999.

[4] P. Zhang, F. Li, and N. Bhatt, "Next-Generation Monitoring, Analysis, and Control for the Future Smart Control Center," *Smart Grid, IEEE Transactions on*, vol. 1, pp. 186–192, Sept 2010.

[5] S. Wang, W. Gao, and A. Meliopoulos, "An Alternative Method for Power System Dynamic State Estimation Based on Unscented Transform," *Power Systems, IEEE Transactions on*, vol. 27, pp. 942–950, May 2012.

[6] E. Ghahremani and I. Kamwa, "Dynamic State Estimation in Power System by Applying the Extended Kalman Filter With Unknown Inputs to Phasor Measurements," *Power Systems, IEEE Transactions on*, vol. 26, pp. 2556–2566, Nov 2011.

[7] A. Singh and B. Pal, "Decentralized Dynamic State Estimation in Power Systems Using Unscented Transformation," *Power Systems, IEEE Transactions on*, vol. 29, pp. 794–804, March 2014.

[8] V. Kekatos and G. Giannakis, "Distributed robust power system state estimation," *Power Systems, IEEE Transactions on*, vol. 28, pp. 1617–1626, May 2013.

[9] E. Ghahremani and I. Kamwa, "Local and wide-area pmu-based decentralized dynamic state estimation in multi-machine power systems," *IEEE Transactions on Power Systems*, vol. 31, pp. 547–562, Jan 2016.

[10] Q. Yang, T. Bi, and J. Wu, "WAMS Implementation in China and the Challenges for Bulk Power System Protection," in *Power Engineering Society General Meeting, 2007. IEEE*, pp. 1–6, June 2007.

[11] G. Anagnostou and B. C. Pal, "Impact of overexcitation limiters on the power system stability margin under stressed conditions," *IEEE Transactions on Power Systems*, vol. 31, pp. 2327–2337, May 2016.

[12] D. Simon, *Optimal state estimation: Kalman, H infinity, and nonlinear approaches*. John Wiley & Sons, 2006.

[13] A. Al-Hussein and A. Haldar, "Unscented kalman filter with unknown input and weighted global iteration for health assessment of large structural systems," *Structural Control and Health Monitoring*, pp. n/a–n/a, 2015.

[14] Z. Luo and H. Fang, "Fault Detection for Nonlinear Systems with Unknown Input," *Asian Journal of Control*, vol. 15, no. 5, pp. 1503–1509, 2013.

[15] M. Witczak, "Unknown Input Observers and Filters," in *Fault Diagnosis and Fault-Tolerant Control Strategies for Non-Linear Systems*, vol. 266 of *Lecture Notes in Electrical Engineering*, pp. 19–56, Springer International Publishing, 2014.

[16] C.-S. Hsieh, "A unified framework for state estimation of nonlinear stochastic systems with unknown inputs," in *Control Conference (ASCC), 2013 9th Asian*, pp. 1–6, June 2013.

[17] B. Pal and B. Chaudhuri, *Robust control in power systems*. Springer, 2006.

[18] "NETS-NYPS 68 Bus System." http://www.sel.eesc.usp.br/ieee/.

[19] G. Terejanu, T. Singh, and P. Scott, "Unscented Kalman Filter/Smoother for a CBRN puff-based dispersion model," in *Information Fusion, 2007 10th International Conference on*, pp. 1–8, July 2007.

[20] S. J. Julier and J. K. Uhlmann, "Unscented filtering and nonlinear estimation," *Proceedings of the IEEE*, vol. 92, pp. 401–422, Mar 2004.

[21] R. Van Der Merwe, *Sigma-point Kalman filters for probabilistic inference in dynamic state-space models*. PhD thesis, Oregon Health & Science University, 2004.

[22] S. Gillijns and B. D. Moor, "Unbiased minimum-variance input and state estimation for linear discrete-time systems," *Automatica*, vol. 43, no. 1, pp. 111 – 116, 2007.

[23] I. Arasaratnam and S. Haykin, "Cubature kalman filters," *IEEE Transactions on Automatic Control*, vol. 54, pp. 1254–1269, June 2009.

[24] I. Arasaratnam, S. Haykin, and T. R. Hurd, "Cubature kalman filtering for continuous-discrete systems: Theory and simulations," *IEEE Transactions on Signal Processing*, vol. 58, pp. 4977–4993, Oct 2010.

[25] N. Zhou, D. Meng, and S. Lu, "Estimation of the dynamic states of synchronous machines using an extended particle filter," vol. 28, pp. 4152–4161, Nov. 2013.

[26] B. Anderson and J. Moore, *Optimal Filtering*. Englewood Cliffs, NJ: Prentice-Hall, 1979.

[27] T. Lefebvre, H. Bruyninckx, and J. D. Schutter, *Nonlinear Kalman Filtering for Force-Controlled Robot Tasks*, vol. 19 of *Springer Tracts in Advanced Robotics*. Springer, 2005.

[28] P. Sauer and A. Pai, *Power System Dynamics and Stability*. Prentice Hall, 1998.

[29] J. Machowski, J. Bialek, and J. Bumby, *Power System Dynamics and Stability*. Wiley, 1997.

[30] Z. Huang, P. Du, D. Kosterev, and S. Yang, "Generator dynamic model validation and parameter calibration using phasor measurements at the point of connection," *IEEE Transactions on Power Systems*, vol. 28, pp. 1939–1949, May 2013.

[31] A. K. Singh and B. C. Pal, "Decentralized control of oscillatory dynamics in power systems using an extended LQR," vol. 31, pp. 1715–1728, May 2016.

[32] L. Fan and Y. Wehbe, "Extended Kalman filtering based real-time dynamic state and parameter estimation using PMU data," *Electric Power Systems Research*, vol. 103, pp. 168 – 177, 2013.

[33] A. G. Phadke and B. Kasztenny, "Synchronized phasor and frequency measurement under transient conditions," *IEEE Transactions on Power Delivery*, vol. 24, pp. 89–95, Jan 2009.

[34] P. Kundur, N. J. Balu, and M. G. Lauby, *Power system stability and control*, vol. 7. McGraw-hill New York, 1994.

[35] K. Padiyar, *Power System Dynamics: Stability and Control*. Anshan, 2004.

[36] "IEEE Standard for Synchrophasor Measurements for Power Systems," *IEEE Std C37.118.1-2011 (Revision of IEEE Std C37.118-2005)*, pp. 1–61, Dec 2011.

[37] "IEEE Standard for Synchrophasor Measurements for Power Systems – Amendment 1: Modification of Selected Performance Requirements," *IEEE Std C37.118.1a-2014 (Amendment to IEEE Std C37.118.1-2011)*, pp. 1–25, April 2014.

[38] A. G. Phadke and J. S. Thorp, *Synchronized phasor measurements and their applications*. Springer Science & Business Media, 2008.

[39] "IEEE Standard Requirements for Instrument Transformers," *IEEE Std C57.13-2008 (Revision of IEEE Std C57.13-1993)*, pp. c1–82, July 2008.

[40] A. Messina, V. Vittal, G. Heydt, and T. Browne, "Nonstationary Approaches to Trend Identification and Denoising of Measured Power System Oscillations," *Power Systems, IEEE Transactions on*, vol. 24, pp. 1798–1807, Nov 2009.

[41] Z. Jiang, S. Miao, and P. Liu, "A Modified Empirical Mode Decomposition Filtering-Based Adaptive Phasor Estimation Algorithm for Removal of Exponentially Decaying DC Offset," *Power Delivery, IEEE Transactions on*, vol. 29, pp. 1326–1334, June 2014.

[42] S. Jha and R. Yadava, "Denoising by Singular Value Decomposition and Its Application to Electronic Nose Data Processing," *Sensors Journal, IEEE*, vol. 11, pp. 35–44, Jan 2011.

[43] U. Dwivedi and S. Singh, "Denoising Techniques With Change-Point Approach for Wavelet-Based Power-Quality Monitoring," *Power Delivery, IEEE Transactions on*, vol. 24, pp. 1719–1727, July 2009.

[44] J. Ren and M. Kezunovic, "An Adaptive Phasor Estimator for Power System Waveforms Containing Transients," *Power Delivery, IEEE Transactions on*, vol. 27, pp. 735–745, April 2012.

[45] D. Shi, D. Tylavsky, and N. Logic, "An Adaptive Method for Detection and Correction of Errors in PMU Measurements," *Smart Grid, IEEE Transactions on*, vol. 3, pp. 1575–1583, Dec 2012.

[46] Q. Zhang, V. Vittal, G. Heydt, N. Logic, and S. Sturgill, "The Integrated Calibration of Synchronized Phasor Measurement Data in Power Transmission Systems," *Power Delivery, IEEE Transactions on*, vol. 26, pp. 2573–2581, Oct 2011.

[47] V. Murugesan, Y. Chakhchoukh, V. Vittal, G. Heydt, N. Logic, and S. Sturgill, "PMU Data Buffering for Power System State Estimators," *Power and Energy Technology Systems Journal, IEEE*, vol. 2, pp. 94–102, 2015.

[48] Q. Zhang, Y. Chakhchoukh, V. Vittal, G. Heydt, N. Logic, and S. Sturgill, "Impact of PMU Measurement Buffer Length on State Estimation and its Optimization," *Power Systems, IEEE Transactions on*, vol. 28, pp. 1657–1665, May 2013.

[49] F. Mahmood, H. Hooshyar, and L. Vanfretti, "A method for extracting steady state components from Syncrophasor data using Kalman Filters," in *Environment and Electrical Engineering (EEEIC), 2015 IEEE 15th International Conference on*, pp. 1498–1503, June 2015.

[50] A. Facchinetti, G. Sparacino, and C. Cobelli, "Online Denoising Method to Handle Intraindividual Variability of Signal-to-Noise Ratio in Continuous Glucose Monitoring," *Biomedical Engineering, IEEE Transactions on*, vol. 58, pp. 2664–2671, Sept 2011.

[51] P. Romano and M. Paolone, "Enhanced Interpolated-DFT for Synchrophasor Estimation in FPGAs: Theory, Implementation, and Validation of a PMU Prototype," *Instrumentation and Measurement, IEEE Transactions on*, vol. 63, pp. 2824–2836, Dec 2014.

[52] D. Belega, D. Macii, and D. Petri, "Fast Synchrophasor Estimation by Means of Frequency-Domain and Time-Domain Algorithms," *Instrumentation and Measurement, IEEE Transactions on*, vol. 63, pp. 388–401, Feb 2014.

[53] A. Roscoe, B. Dickerson, and K. Martin, "Filter Design Masks for C37.118.1a-Compliant Frequency-Tracking and Fixed-Filter M-Class Phasor Measurement Units," *Instrumentation and Measurement, IEEE Transactions on*, vol. 64, pp. 2096–2107, Aug 2015.

[54] A. Roscoe, "Exploring the relative performance of frequency-tracking and fixed-filter phasor measurement unit algorithms under c37.118 test procedures, the effects of interharmonics, and initial attempts at merging p-class response with m-class filtering," *Instrumentation and Measurement, IEEE Transactions on*, vol. 62, pp. 2140–2153, Aug 2013.

[55] P. Castello, J. Liu, C. Muscas, P. Pegoraro, F. Ponci, and A. Monti, "A Fast and Accurate PMU Algorithm for P + M Class Measurement of Synchrophasor and Frequency," *Instrumentation and Measurement, IEEE Transactions on*, vol. 63, pp. 2837–2845, Dec 2014.

[56] P. Romano and M. Paolone, "An enhanced interpolated-modulated sliding DFT for high reporting rate PMUs," in *Applied Measurements for Power Systems Proceedings (AMPS), 2014 IEEE International Workshop on*, pp. 1–6, Sept 2014.

Georgios Anagnostou (M'17) was born in Athens, Greece. He received the Diploma in Electrical and Computer Engineering from the National Technical University of Athens (NTUA), Athens, Greece, the M.Sc. degree in Sustainable Energy Futures from Imperial College London, London, United Kingdom, and the Ph.D. degree in Electrical Engineering from Imperial College London, London, United Kingdom in 2011, 2012, and 2016, respectively. His current research interests include power system dynamics and control, dynamic security assessment, dynamic state estimation, and renewable energy based generation. Dr. Anagnostou is a member of the Technical Chamber of Greece.

Bikash C. Pal (M'00-SM'02-F'13) received the B.E.E.(with honours) degree from Jadavpur University, Calcutta, India, the M.E. degree from the Indian Institute of Science, Bangalore, India, and the Ph.D. degree from Imperial College London, London, U.K, in 1990, 1992, and 1999, respectively, all in electrical engineering. Currently, he is a Professor in the Department of Electrical and Electronic Engineering, Imperial College London, London, U.K. His current research interests include state estimation, power system dynamics, and flexible AC transmission system controllers. He is the Editor-in-Chief of IEEE TRANSACTIONS ON SUSTAINABLE ENERGY and a Fellow of the IEEE for his contribution to power system stability and control.